IIETA International Information and Engineering Technology Association
Advancing the World of Information and Engineering

Traitement du Signal
Vol. 39, No. 1, February, 2022, pp. 381-387
Journal homepage: http://iieta.org/journals/ts

Analysis on Chlorophyll Diagnosis of Wheat Leaves Based on Digital Image Processing and Feature Selection

Yufei Song, Shiwu Li, Zhiguo Liu*, Yuekui Zhang, Nan Shen

School of Computer Science & Engineering, Shijiazhuang University, Shijiazhuang 050035, China

Corresponding Author Email: 1102192@sjzc.edu.cn

https://doi.org/10.18280/ts.390140

Received: 29 October 2021
Accepted: 5 January 2022

Keywords:
image processing, color feature selection, SPAD 502 plus chlorophyll meter, machine learning

ABSTRACT

Crop nutrition measurement is of great significance in agricultural practice, especially in variable rate fertilization. The chlorophyll content, an important indicator of nitrogen nutrition in crops, largely depends on crop growth and development, photosynthesis, and crop yield, and plays an important role in the monitoring of crop growth. This paper tries to detect the chlorophyll content of wheat quickly, using the digital image processing technology. Specifically, a feature selection method was developed based on wrapper and light gradient boosting machine (LGBM), and combined with logistic regression (LR) to predict the chlorophyll content of wheat. The results show that: the optimal model is the combination between the 17 image evaluation indices screened by LGBM and the LR prediction model; the optimal results were coefficient of determination (R2) of 0.728, and root mean square error (RMSE) of 4.979. The optimal model can predict the chlorophyll content of wheat accurately based on digital images in field prototype.

1. INTRODUCTION

Chlorophyll, the main pigment for plant photosynthesis, is an important indicator of the health state and nutritional content of plants [1]. By measuring the chlorophyll content, the health state and nitrogen content of a plant can be assessed directly [2, 3].

In the past few decades, digital imaging provides a fast, non-destructive, and high-throughput determination tool for chlorophyll content [4]. Many color features of leaves, which are captured by rigorous experimental devices (e.g., scanners) have been shown to be highly correlated with the chlorophyll content of plants [5-12]. Although the previous experimental results of chlorophyll assessment are quite accurate, the samples are mostly collected in the lab environment.

In field prototype, it is challenging to acquire images by digital cameras for chlorophyll estimation. For example, some color features from the red-green-blue (RGB) space can be influenced by the ambient light. Numerous attempts have been made to overcome the problem. Vesali et al. [4] reduced the interference of environmental conditions through contact imaging. Kawashima and Nakatani [13] Wang et al. [14] took pictures with a digital camera on overcast days. Riccardi et al. [15] directly captured images directly in natural light from field prototype using a digital camera on sunny days. To facilitate image acquisition, leaves were pressed on a white graduated support plane, without detaching from the plant. The chlorophyll content of plants can be estimated effectively, based on the features of the RGB color space in sunny weather.

In terms of feature selection and image modeling, most of the previous image-based assessment tools for plant chlorophyll content only consider the RGB color space, and resort to least squares regression [10, 15]. Thanks to the development of digital imaging and data mining, other color spaces and machine learning algorithms are being introduced to chlorophyll diagnosis. For instance, the leaf images of sugar beet and potato are used to extract the color features L, G, and B, and artificial neural networks (ANNs) are employed to evaluate the chlorophyll content [5, 9]. Vesali et al. [4] extracted four features from the RGB and hue-saturation-intensity (HSI) color spaces, including LF, H, SH, and SCr, and established a neural network for estimating chlorophyll content. Amin and Awang [16] extracted 36 features from the RGB color space, and determined the nutritional status of Napier grass with the k-nearest neighbors algorithm (KNN). Yang [17] relied on the KNN and extreme gradient boosting (XGBoost) to estimate the chlorophyll content of maize leaves at different growth stages.

Nevertheless, more features do not necessarily lead to better estimation. Due to the limitations of the imaging technology, the information acquired by digital camera is limited. The color features of wheat leaves extracted from digital images may have a high collinearity [18]. This calls for feature selection in multivariate data analysis. The effective selection of features will provide a better understanding of the data generation process. The best feature set needs to be selected based on prediction ability [19-22].

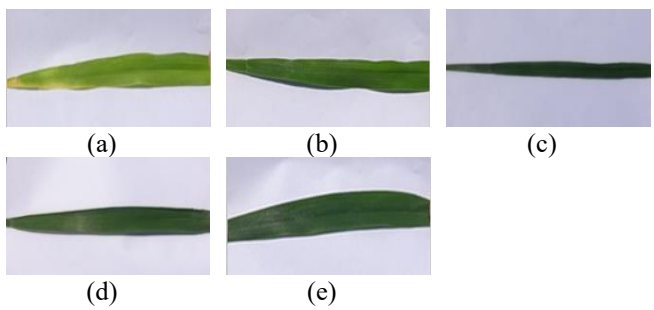

Figure 1. Wheat leaf images

The above analysis shows that digital image processing can build chlorophyll prediction models quickly and accurately. However, there is not yet a good feature selection model for the various feature indices of color images. Focusing on the color features of digital wheat images, this paper devises a feature selection method based on wrapper and light gradient boosting machine (LGBM), and combines the method with machine learning algorithm to develop a diagnosis model for chlorophyll nutrition of wheat.

2. DATA ACQUISITION AND IMAGE PROCESSING

2.1 Acquisition of image data and SPAD value

(1) Overview of experimental area

The experimental area (N: 38°46′24.90; E: 115°32′33.23) lies in the demonstration field base of Hebei Agricultural University, in Qingyuan District, Baoding, northern China's Hebei Province. According to the experimental design, the area was divided into 15 plots numbered 1-15. In each plot, nitrogen was applied at five different levels 0 kg/hm^2 (N0), 100 kg/hm^2 (N100), 180 kg/hm^2 (N180), 225 kg/hm^2 (N255), and 330 kg/hm^2 (N330). Table 1 shows the correspondence between plots and nitrogen application levels.

(2) Instruments

The images were acquired by a Sony FDR-AXP35 4K high definition (HD) camera, which adopts a 1/2.3-inch Exmor R CMOS image sensor and a Carl Zeiss Vario-Sonnar T* lens. The camera supports optical anti-shake mode and 10x optical zoom. Each image being captured has 8.29 million effective pixels. The maximum number of pixels can reach 18.9 million. The image resolution is 3,840×2,140. For convenience, the aperture priority mode was selected, along with its automatic white balance, focusing mode, shutter speed, and sensitivity.

The portable chlorophyll meter is a non-destructive measuring instrument of plant chlorophyll content. Owing to its real-time performance, efficiency, and portability, the instrument has been widely adopted to measure chlorophyll in living leaves. The SPAD value measured by the portable chlorophyll meter is highly consistent with the chlorophyll content of plant leaves. Here, a Minolta SPAD 502 plus portable chlorophyll meter is adopted for chlorophyll measurement.

(3) Image acquisition

Jointing is a key stage in the growth of wheat. The crop is fertilized quickly in this stage, due to the fast absorption and accumulation of nutrients. Taking jointing wheat as the research object, this paper collects wheat images in field environment.

Extreme weather was avoided during image acquisition. To prevent unstable light, the shooting time was arranged between 10:00 and 14:00 on a sunny and cloudless day. In-situ sampling was carried out without damaging the leaves.

During sampling, the camera lens was perpendicular to 30cm above the wheat leaves. To avoid environmental interference and facilitate target extraction, a white background plate was placed close to the leaves before image shooting. In the experimental area, 30 wheat leaves of uniform growth state were randomly selected from each plot, producing a total of 450 leaf images. Figure 1 presents the acquired leaf images, and Table 2 reports the correspondence between images and nitrogen application levels.

Table 1. Correspondence between plots and nitrogen application levels

Plot number	Nitrogen application level (kg/hm^2)				
	0	100	180	255	330
1, 8, 10				※	
2, 9, 13		※			
3, 5, 12					※
4, 7, 14			※		
6, 11, 15	※				

Table 2. Correspondence between images and nitrogen application levels

Image number	Plot number	Nitrogen application level	Number of images
(a)	6	N0	90
(b)	9	N100	90
(c)	4	N180	90
(d)	1	N255	90
(e)	5	N330	90

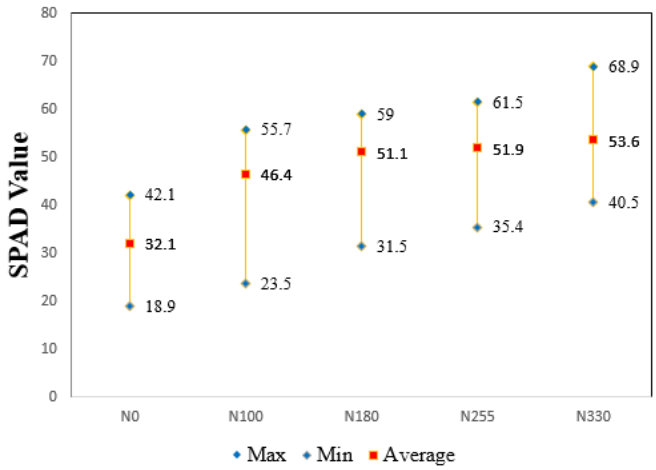

Figure 2. SPAD distribution in different plots with different nitrogen application levels

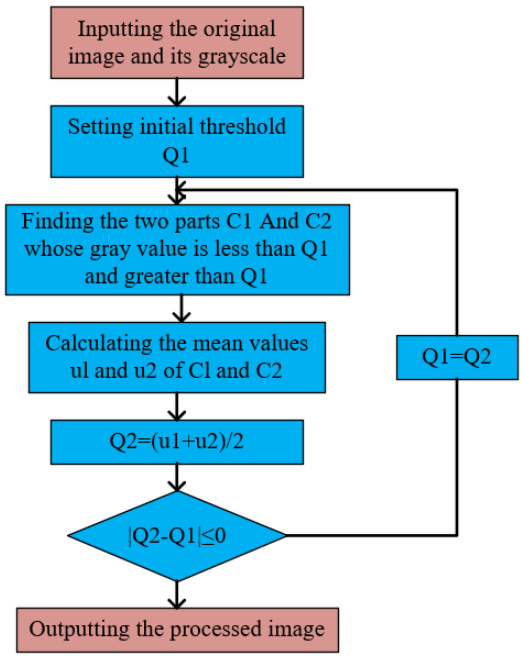

Figure 3. Flow of image processing

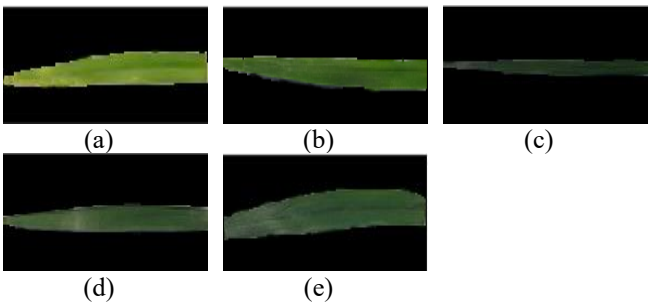

Figure 4. Results of image segmentation

(4) Acquisition of SPAD value

The chlorophyll content of wheat leaves was also obtained through the experiments. After taking each image, the portable chlorophyll meter was immediately clamped onto the leaf tip, leaf, and leaf base, and each part was measured three times, yielding nine measured values. The mean of the nine values was taken as the chlorophyll content of the leaf. Figure 2 shows the SPAD distribution in different plots with different nitrogen application levels.

2.2 Target extraction

Target extraction aims to separate wheat leaves from the collected images. As mentioned above, each image was shot in the field with a whiteboard close to the leaves. The gray features of the image can be used for the separation, due to the large difference between the leaves and the background. Hence, the simple and efficient iterative thresholding was adopted for target extraction. As shown in Figure 3, the target extraction is realized in the following steps:

Step 1. Compute the minimum A0 and maximum A1 of gray value in the original image, and set up the initial threshold Q1=(A0+A1)/2.

Step 2. Segment the image with the initial threshold Q1, and divide the gray values smaller and greater than Q1 into two parts: C1 and C2.

Step 3. Compute the mean gray values of C1 and C2, and assign the results to μ1 and μ2.

Step 4. Compute the new threshold Q2=(μ1+μ2)/2.

Step 5. If |Q2-Q1|≤0, then take Q2 as the optimal threshold; Otherwise, make Q1=Q2 and repeat Steps (2)-(4) until the end of iterations.

The output binary image is generated by multiplying the pixels of the original image. The extracted targets are displayed in Figure 4.

2.3 Generation of image features

Each target image may contain various evaluation indices related to the prediction of chlorophyll content in wheat. The indices selected for mathematical transformation constitute a set of evaluation indices. In most literature, the image evaluation indices selected for wheat chlorophyll content diagnosis concentrate in the RGB color space, and work well in the prediction of chlorophyll content in wheat. Recently, the HSI color space, L*a*b* color space, normalized RGB color space, dark green color index (DGCI), and normalized redness intensity (NRI) have also shown very good results in the diagnosis of wheat chlorophyll content. Therefore, 39 image features were combined according to the color spaces mentioned in recent studies into an image feature set. The RGB color space can be converted to HSI color space, XYZ color space, and L*a*b* color space by formulas (1)-(7).

$$H = \begin{cases} \theta & (G \geq B) \\ 2\pi - \theta & (G < B) \end{cases} \tag{1}$$

where, $\theta = \arccos\left\{\frac{[(R-G)+(R-B)]/2}{[(R-G)^2+(R-B)(B-G)]^{1/2}}\right\}$.

$$\mathrm{S} = 1 - \frac{3}{R+G+B} \cdot \min(R, \mathrm{G}, \mathrm{B}) \tag{2}$$

$$\mathrm{I} = \frac{(R+B+G)}{3} \tag{3}$$

$$\begin{bmatrix} X \\ Y \\ Z \end{bmatrix} = \begin{bmatrix} 0.4124 & 0.3576 & 0.1805 \\ 0.2126 & 0.7152 & 0.0722 \\ 0.0193 & 0.1192 & 0.9505 \end{bmatrix} * \begin{bmatrix} R \\ G \\ B \end{bmatrix} \tag{4}$$
$$0 \leq (\mathrm{R}, \mathrm{G}, \mathrm{B}) \leq 1$$

$$L = \begin{cases} 116.0 \times f(Y/Y_n) - 16.0 & if\ Y/Y_n > 0.008856 \\ 903.3 \times (Y/Y_n) & if\ Y/Y_n \leq 0.008856 \end{cases} \tag{5}$$

$$a^* = 500[f(X/X_n) - f(Y/Y_n)] \tag{6}$$

$$b^* = 200[f(Y/Y_n) - f(Z/Z_n)] \tag{7}$$

where,

$$f(t) = \begin{cases} \frac{1}{3}(\frac{6}{29})^3 t + \frac{4}{29} & if\ t \leq 0.008856 \\ t^{\frac{1}{3}} & if\ t > 0.008856 \end{cases};$$

X_n, Y_n, and Z_n indicate the tristimulus values of the reference white point.

From each of the twelve color channels (R, G, B, H, S, I, X, Y, Z, L, a* and b*), an average color feature was extracted by formula (8). To reduce the influence of illumination on images, the image in the RGB channels was normalized by formulas (9)-(11).

$$\mathrm{Mean}(\mu) = \frac{1}{MN}\sum_{i=1}^{M}\sum_{j=1}^{N} P(i,j) \tag{8}$$

$$r = \frac{R}{\sqrt{R^2+G^2+B^2}} \tag{9}$$

$$g = \frac{G}{\sqrt{R^2+G^2+B^2}} \tag{10}$$

$$b = \frac{B}{\sqrt{R^2+G^2+B^2}} \tag{11}$$

where, M, N, and $P(i, j)$ are the dimension of the image matrix, the total number of pixels in the image, and the color value of the pixel in the i-th column and j-th row, respectively.

3. FEATURE SELECTION AND MODELING

Most of the previous studies on wheat chlorophyll content focus on the extraction of different image features. Only a few scholars tackled the screening of the best feature subset of images. The importance of feature selection is self-evident: the selection of good features not only reduces the difficulty of

learning, but also eliminates the effect of noise on the model. From the constructed set of image features, a subset of image features needs to be selected by an appropriate algorithm, facilitating the diagnosis of chlorophyll content in wheat leaves.

3.1 Wrapper-based feature selection algorithm

Once the evaluation index set of the target image is established, the first step is to implement recursive feature elimination (RFE), and adopt the random forest model. The 39 original image features are used for pre-training. Each feature is assigned a weight, and the feature importance is outputted. In the second step, the cross-validation version of RFE (RFECV) performs the RFE by eliminating one feature at a time through 5-fold cross-validation. Hence, the best subset of image features is screened automatically. The screened results are displayed in Table 3.

Table 3. Results of wrapper-based feature selection

Features	Importance	Rank	Features	Importance	Rank
R	0.0208	15	G+B	0.0234	22
G	0.0224	21	G-B	0.0223	3
B	0.0237	1	R+G-B	0.0234	14
r	0.0252	1	G/R	0.0248	9
g	0.0254	1	G/B	0.0234	11
b	0.0260	1	(R-B)/(R+B)	0.0243	16
H	0.0356	1	(R-G)/(R+G)	0.0237	18
S	0.0305	1	(G-B)/(G+B)	0.0231	1
I	0.0215	20	(R-B)/(R+G+B)	0.0239	1
L	0.0225	19	(R-G)/(R+G+B)	0.0263	6
a*	0.0259	1	(G-B)/(R+G+B)	0.0239	12
b*	0.0256	2	R-G-B	0.0281	1
X	0.0333	1	R-G	0.0258	5
Y	0.0367	1	R-B	0.0263	1
Z	0.0365	1	G/R	0.0249	1
R-G-B	0.0261	1	NIR	0.0268	1
R-G	0.0294	1	NIG	0.0244	7
R-B	0.0246	8	NIB	0.0258	13
R+G	0.0205	10	DGCI	0.0211	17
R+B	0.0224	4			

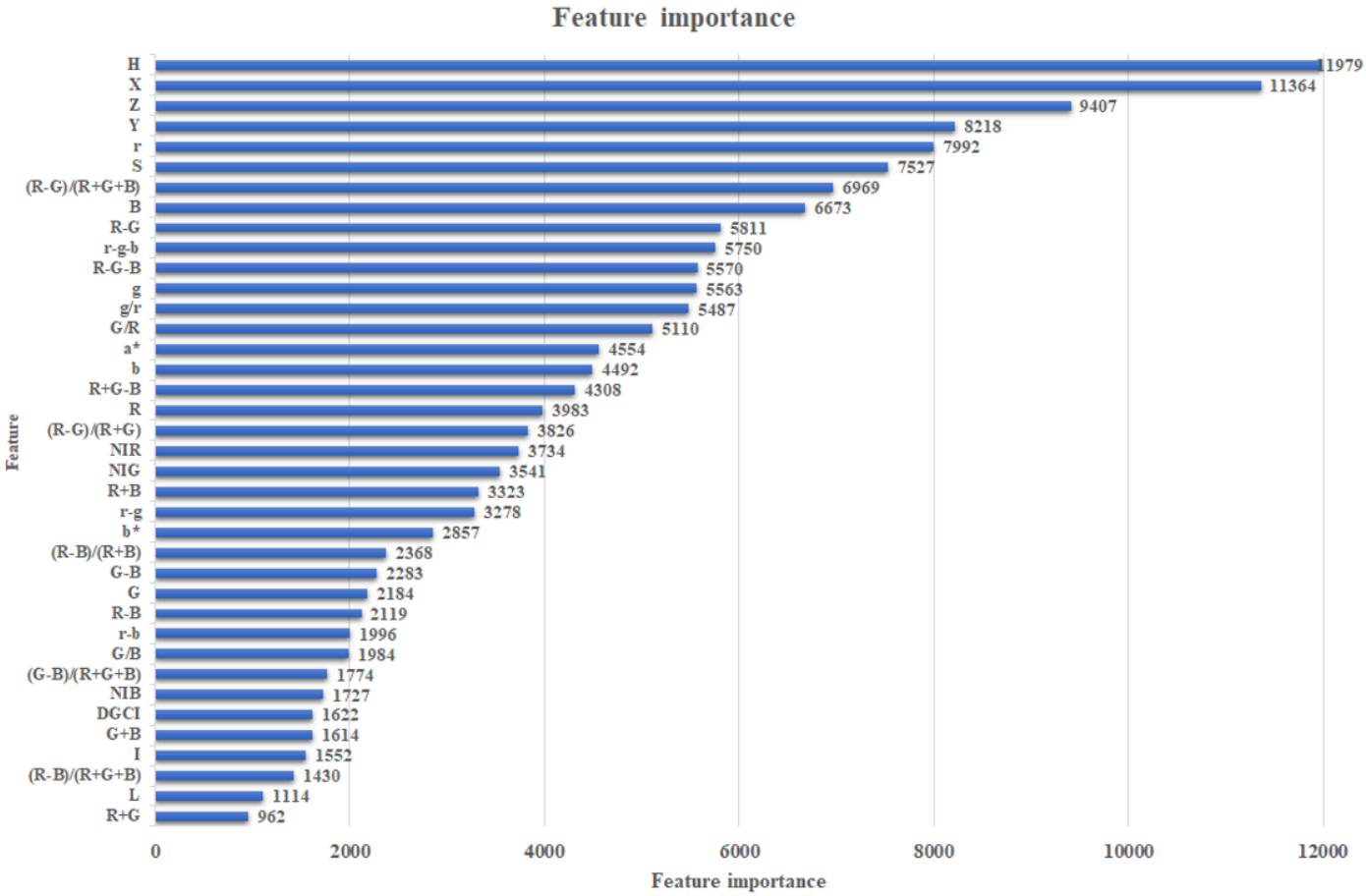

Figure 5. Results of LGBM-based feature selection

Table 4. Main parameters of each model

Model	Parameter	Model	Parameter
XGBoost	'clf__max_depth':[10] 'clf__min_child_weight':[6] 'clf__booster':('gbtree','gblinear') 'clf__subsample':[0.5] 'clf__colsample_bytree':(0.4,0.5)	RF	'clf__n_estimators': [10, 20, 50] 'clf__max_features':[None,1, 2] 'clf__max_depth': [1,2,5,7,9]
KNN	'clf__n_neighbors':[5, 10, 15, 25, 30] 'clf__weights':['uniform','distance']	NN	'clf__alpha':[0.001,0.01,0.1,1,10,100] 'clf__hidden_layer_sizes':[(5),(10,10)] 'clf__activation': ['relu', 'tanh'] 'clf__learning_rate':['constant','invscaling']}

3.2 LGBM-based feature selection algorithm

Another option is to integrates gradient boosted decision trees (GBDTs) for index screening. Firstly, the top-K image features are identified automatically, and the features that may be the best segmentation points are selected by voting. The feature importance is computed by setting the mean gain based on the parameter "gain". Then, the parameter "split" is used to judge whether the index is the optimal segmentation point. After that, only the features filtered by each model are merged, and the output image forms different feature subsets with the cliff part as the boundary. Finally, the best image feature subset is found according to the results. The results of LGBM-based feature selection are displayed in Figure 5.

3.3 Diagnostic model for leaf chlorophyll content

After identifying the subset of the best image features, the diagnosis model of wheat leaf chlorophyll content was established by five machine learning algorithms, such as logistic regression (LR), XGboost, KNN, random forest (RF), and nearest neighbor (NN). The main parameters of each algorithm are shown in Table 4. The diagnosis model measures the difference between the estimated value and the real value with the coefficient of determination (R^2). The model accuracy was measured by root mean square error (RMSE). The results are shown in Table 5.

(1) RFECV-based feature selection

The model analysis was carried out based on the 18 image features screened by the RFECV. Through dimensionality reduction, the size of the training set is reduced, which affects the accuracy of NN and KNN to a certain extent. Meanwhile, the accuracy of LR, XGBoost and RF was improved, compared with the training model of the original data. Hence, the selected feature subset has a certain effect in the diagnostic modeling and analysis of chlorophyll content in wheat leaves. The results of RFECV-based feature selection are shown in Table 6.

Contrary to the current technical development, the classification effect of the NN was not as good as that of any other classifier. It has been proved that the NN will be overfitted in some classification or regression problems with too much noise. The attributes with relatively great values have an immense impact on the RF. That is why the attribute weights computed by the RF is not necessarily credible. In this paper, the features are constructed based on the combined mode, and are relatively salient. Thus, LR and other models can avoid overfitting to a certain extent, and perform relatively well in this experiment.

(2) LGBM-based feature selection

The importance of each image feature was calculated by the LGBM-based feature selection algorithm. Taking the cliff phenomenon as the boundary, four feature subsets were selected as the training data to fit the model. With the growing number of features in Groups 1-3, the fitting effect of most models got better. As the number of features rose to 20 (Group 4), the fitting effect of the model was weakened to a certain extent. The results of the LR are presented in Table 7.

LR achieved the best result, with R^2 of 0.727 and RMSE of 4.979. The optimal prediction model is displayed in Figure 6. Compared with those obtained by the wrapper-based feature selection algorithm, the 17 image features chosen by the LGBM-based feature selection algorithm form the best set of image features.

Table 5. Results of original image feature modeling

Model	R^2	RMSE
LR	0.718	5.065
XGBoost	0.621	5.89
KNN	0.667	5.543
RF	0.709	5.147
NN	0.726	5.074

Table 6. Results of RFECV-based feature selection

Model	R^2	RMSE
LR	0.727	5.001
XGBoost	0.681	5.275
KNN	0.619	5.923
RF	0.713	5.202
NN	0.351	5.097

Table 7. Results of LGBM-based feature selection

LR/Score	R^2	RMSE
First	0.709	5.182
Second	0.725	5.022
Third	0.728	4.979
Fourth	0.721	5.072

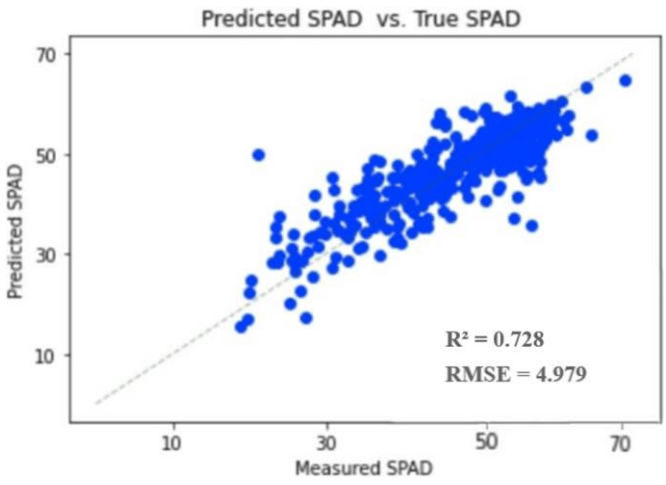

Figure 6. Optimal prediction model

4. CONCLUSIONS

Chlorophyll is an important measure of plant nitrogen content and other health indices. This paper studies the relationship between leaf color features and chlorophyll content at the jointing stage of wheat under different nitrogen application levels. A total of 39 image features were extracted from different color spaces, and sorted and screened by wrapper and LGBM. Then, LR, XGBoost, KNN, RF, and NN were combined to form the estimation model for the relationship between color features and chlorophyll content. Experimental results show that the best model of leaf chlorophyll in the field prototype is the prediction model coupling LGBM with LR. The optimal results are R^2=0.728 and RMSE=4.979.

Although the estimation results are not as accurate as the existing alternatives (SPAD instrument, spectrometer, hyperspectral equipment, etc.), our model can be directly used in field prototype to yield effective estimation results. However, the research object is limited to Jimai 22. The performance of our model on other wheat varieties needs to be further verified. In addition, this paper only estimates the chlorophyll content of a single leaf of wheat. The future research will estimate the chlorophyll content of the wheat population, which has better application value.

ACKNOWLEDGMENTS

This paper was supported by the Scientific Science and Technology Research Projects of Universities in Hebei, China (Grant No.: QN2021409), and the Foundation for Doctoral Research of Shijiazhuang University, China (Grant No.: 21BS017).

REFERENCES

[1] Steele, M.R., Gitelson, A.A., Rundquist, D.C. (2008). A comparison of two techniques for nondestructive measurement of chlorophyll content in grapevine leaves. Agronomy Journal, 100(3): 779-782. https://doi.org/10.2134/agronj2007.0254N

[2] Yadav, S.P., Ibaraki, Y., Dutta Gupta, S. (2010). Estimation of the chlorophyll content of micropropagated potato plants using RGB based image analysis. Plant Cell, Tissue and Organ Culture (PCTOC), 100(2): 183-188. https://doi.org/10.1007/s11240-009-9635-6

[3] Muñoz-Huerta, R.F., Guevara-Gonzalez, R.G., Contreras-Medina, L.M., Torres-Pacheco, I., Prado-Olivarez, J., Ocampo-Velazquez, R.V. (2013). A review of methods for sensing the nitrogen status in plants: advantages, disadvantages and recent advances. sensors, 13(8): 10823-10843. https://doi.org/10.3390/s130810823

[4] Vesali, F., Omid, M., Kaleita, A., Mobli, H. (2015). Development of an android app to estimate chlorophyll content of corn leaves based on contact imaging. Computers and Electronics in Agriculture, 116: 211-220. https://doi.org/10.1016/j.compag.2015.06.012

[5] Moghaddam, P.A., Derafshi, M.H., Shirzad, V. (2011). Estimation of single leaf chlorophyll content in sugar beet using machine vision. Turkish Journal of Agriculture and Forestry, 35(6): 563-568. https://doi.org/10.3906/tar-0909-393

[6] Dey, A.K., Sharma, M., Meshram, M.R. (2016). An analysis of leaf chlorophyll measurement method using chlorophyll meter and image processing technique. Procedia Computer Science, 85: 286-292. https://doi.org/10.1016/j.procs.2016.05.235

[7] Yuan, Y., Chen, L., Li, M., et al., (2016). Diagnosis of nitrogen nutrition of rice based on image processing of visible light. In 2016 IEEE International Conference on Functional-Structural Plant Growth Modeling, Simulation, Visualization and Applications (FSPMA), Qingdao, China, pp. 228-232. https://doi.org/10.1109/FSPMA.2016.7818311

[8] Reyes, J.F., Correa, C., Zuniga, J. (2017). Reliability of different color spaces to estimate nitrogen SPAD values in maize. Computers and Electronics in Agriculture, 143: 14-22. https://doi.org/10.1016/j.compag.2017.09.032

[9] Dutta Gupta, S., Pattanayak, A.K. (2017). Intelligent image analysis (IIA) using artificial neural network (ANN) for non-invasive estimation of chlorophyll content in micropropagated plants of potato. Vitro Cellular & Developmental Biology-Plant, 53(6): 520-526. https://doi.org/10.1007/s11627-017-9825-6

[10] Borhan, M.S., Panigrahi, S., Satter, M.A., Gu, H. (2017). Evaluation of computer imaging technique for predicting the SPAD readings in potato leaves. Information Processing in Agriculture, 4(4): 275-282. https://doi.org/10.1016/j.inpa.2017.07.005

[11] Agarwal, A., Gupta, S.D. (2018). Assessment of spinach seedling health status and chlorophyll content by multivariate data analysis and multiple linear regression of leaf image features. Computers and Electronics in Agriculture, 152: 281-289. https://doi.org/10.1016/j.compag.2018.06.048

[12] Tushar, S.N.B., Pal, T., Das, S.S., Imam, M.M., Reja, M.I. (2019). A low-cost image processing based technique to estimate chlorophyll in winter wheat. In 2019 International Conference on Electrical, Computer and Communication Engineering (ECCE), Cox'sBazar, Bangladesh, pp. 1-6. https://doi.org/10.1109/ECACE.2019.8679462

[13] Kawashima, S., Nakatani, M. (1998). An algorithm for estimating chlorophyll content in leaves using a video camera. Annals of Botany, 81(1): 49-54. https://doi.org/10.1006/anbo.1997.0544

[14] Wang, Y., Wang, D., Shi, P., Omasa, K. (2014). Estimating rice chlorophyll content and leaf nitrogen concentration with a digital still color camera under natural light. Plant methods, 10(1): 36. https://doi.org/10.1186/1746-4811-10-36

[15] Riccardi, M., Mele, G., Pulvento, C., Lavini, A., d'Andria, R., Jacobsen, S.E. (2014). Non-destructive evaluation of chlorophyll content in quinoa and amaranth leaves by simple and multiple regression analysis of RGB image components. Photosynthesis Research, 120(3): 263-272. https://doi.org/10.1007/s11120-014-9970-2

[16] Amin, S.R.M., Awang, R. (2018). Automated detection of nitrogen status on plants: Performance of image processing techniques. In 2018 IEEE Student Conference on Research and Development (SCOReD), Selangor, Malaysia, pp. 1-4. https://doi.org/10.1109/SCORED.2018.8711334

[17] Yang, J. (2019). Remote sensing model of physiological parameters of summer maize at different growth stages based on machine learning algorithms. Master thesis. Northwest A&F University.
[18] Song, Y., Teng, G., Yuan, Y., Liu, T., Sun, Z. (2021). Assessment of wheat chlorophyll content by the multiple linear regression of leaf image features. Information Processing in Agriculture, 8(2): 232-243. https://doi.org/10.1016/j.inpa.2020.05.002
[19] Guyon, I., Elisseeff, A. (2003). An introduction to variable and feature selection. Journal of machine learning research, 3(Mar): 1157-1182.
[20] Saberioon, M.M., Amin, M.S.M., Anuar, A.R., Gholizadeh, A., Wayayok, A., Khairunniza-Bejo, S. (2014). Assessment of rice leaf chlorophyll content using visible bands at different growth stages at both the leaf and canopy scale. International Journal of Applied Earth Observation and Geoinformation, 32: 35-45. https://doi.org/10.1016/j.jag.2014.03.018
[21] Marenco, R.A., Antezana-Vera, S.A., Nascimento, H.C.S. (2009). Relationship between specific leaf area, leaf thickness, leaf water content and SPAD-502 readings in six Amazonian tree species. Photosynthetica, 47(2): 184-190. https://doi.org/10.1007/s11099-009-0031-6
[22] Zhou, L., Yuan, Y., Song, Y., Wang, B. (2017). Research on estimation of wheat chlorophyll using image processing technology. MATEC Web of Conferences, 128: 01007. https://doi.org/10.1051/matecconf/201712801007